polymer papers

Time-resolved synchrotron X-ray study of chain-folded crystallization of long paraffins

Goran Ungar* and Andrew Keller
H. H. Wills Physics Laboratory, University of Bristol, Tyndall Avenue, Bristol BS8 1TL, UK
(Received 13 May 1986)

The examination of the crystallization of strictly uniform ultra-long n-alkanes was resumed with the view of exploring the onset of chain-folding, as laid out previously in ref. 1. The present study, largely on $C_{246}H_{494}$, centred on the initial stages of crystallization in the melt, registered *in situ* by time-resolved small-angle X-ray scattering using a synchrotron X-ray source. The salient new feature was the identification of transient initial fold lengths which were non-integer fractions (NIF) of the chain length. This NIF structure transforms subsequently into forms with integer fraction (IF) fold lengths. In the present study the latter have the extended chain (E) and once-folded (F2) configurations, while NIF has a fold length between the two. The NIF→IF transformation occurs either by lamellar thickening or thinning, or by both. It was found that the NIF state had a more disordered layer surface as compared to the final E and F2 structures, the latter being the states on which the conclusions in ref. 1 had been drawn, which accordingly should apply to the transformed material. Implications of these and several other findings for some central issues in polymer crystallization are briefly discussed. The existence of an initial NIF phase focusses attention to the importance of the fastest kinetic pathway as the determining factor for chain-folded crystal growth with particular attention to the initial chain deposition probability, a line made accessible by the present alkanes.

(Keywords: crystallization; small-angle X-ray scattering; paraffins)

INTRODUCTION

Background

In a previous publication[1] we announced the first results of a new line of investigation aimed at the elucidation of some of the basic issues of chain-folded crystallization: the onset of chain folding with increasing chain length of the molecule and the nature of the fold. This has become possible thanks to the availability of n-alkanes of strictly uniform length—on the standards of traditional organic chemistry—up to $C_{390}H_{782}$, i.e. chain lengths corresponding to low molecular weight polyethylenes[2].

In this second paper on the subject we proceed with the announcement of some subsequent findings, we believe of qualitative novelty.

First, the main points of the previous announcement will need recapitulating together with newly arising relevant references.

The main points of ref. 1 are as follows:

(i) For the lamellar crystals, as familiar in paraffin crystallization, chain-folded (as opposed to extended chain) crystallization sets in with $C_{150}H_{302}$ (more precisely this compound folds, while the next lowest $C_{102}H_{206}$, investigated earlier, does not).

(ii) The fold length (l) is a function of crystallization temperature T_c or, more precisely, of supercooling ΔT, higher T_c yielding higher l values.

(iii) The fold length is quantized, the chains complete almost exactly one, two, three and four folds up to the longest chain $C_{390}H_{782}$ examined so far.

(iv) It follows from (iii) that the methyl chain ends tend to be at the lamellar surface.

(v) The folds in question must be sharp comprising only a very few chain members, and correspondingly folding must be in the main adjacently re-entrant. (i–v) were found to hold for crystallization both from the melt and from solution.

The above information was obtained from measurement of l either by low frequency Raman (longitudinal acoustic mode, LAM)) or by small-angle X-ray scattering (SAXS) methods, in the latter case due allowance being made for chain inclination (see also below), and by a combination of both techniques, where these l values were compared with the length of the chain (L) which is accurately known.

At this point we wish to give due recognition to historical precedents. Foremost of these are the remarkable SAXS[3] and morphological[4] studies on low molecular weight polyethylene oxides (PEO) with (on polymeric standards) narrow molecular weight distributions. While the principal findings in these works for PEO are closely similar to those now identified for n-alkanes regarding points (i–iv) above, the rather specific end-groups involved have stood in the way of broader generalizations of effects (iii) and (iv); further, the narrow, but still finite, spread of chain lengths prevented point (v) to be forcefully made. This present work, far from reducing the importance of these precedents on PEO, bear out their universal validity to an extent not assertable previously.

In contrast to the above, are past or current works on purely methylene based chains which do *not* bear out our own principal conclusions, or at least not all. Amongst these are studies on sharp fractions of low molecular weight polyethylenes[5,6]. Here no quantized, only continuously varying l values were observed, yet there were discontinuities in crystal growth rates[6], which by

*On leave from the Ruder Boskovic Institute, Zagreb, Yugoslavia.

0032-3861/86/121835-10$03.00

analogy to PEO[7] and to our current works[8], can be taken as pointers to discontinuities in l with T_c (or ΔT). Even closer to our present work are some other parallel investigations on model alkanes[9]. Here strictly uniform n-alkanes (together with long cyclic alkanes) were synthesized by a route different from that of Whiting *et al.* involving a separation of end products (a step which the Whiting synthesis avoids) up to $C_{384}H_{770}$. Our points (i) and (ii) were affirmed independently, but not the rest, i.e. there was no quantization of l (our point (iii)). The latter precludes making points (iv) and (v) with all their consequences. Instead, the authors draw inferences about a disordered fold surface along lines familiar from studies on polyethylene.

The origin of the differences, such as there are, is not clear. The issues are central and the resolving of the differences is clearly required. Very relevant to the subject, and to the above mentioned apparently conflicting findings, are recent results on triblock oligomers of oxyethylene of strictly uniform length with terminal methyl groups[10]. Here primary crystallization yielded non-integer SAXS long spacing values but fully extended or, more significantly for the present purpose, accurately once-folded structure could be inferred as resulting from annealing.

The novelty of the work in the present paper rests both on the subject matter studied and on the experimental methods used. Regarding the subject matter, this consists of registering and following l in the course of crystallization *in situ*, i.e. at elevated temperatures, as opposed to registering it at the end of crystallization after cooling to room temperature as done in ref. 1. Regarding technique, it accomplishes the above using a SAXS method with a synchrotron source. In this respect it demonstrates the capabilities, in fact the necessity, of this kind of high intensity X-ray source for polymer crystallization studies, which from the point of view of methodology is a topic in its own right. In view of their timeliness the present announcement of the new results has been brought ahead of the publication of a comprehensive account underlying ref. 1.

Assignment of l *values*

In ref. 1 l values were determined in the first place by Raman spectroscopy, relating frequency ν_1 of the first-order LAM mode with coherently vibrating stem length l through the formula[11]:

$$\nu_1 = \frac{1}{2l}\left(\frac{E}{\rho}\right)^{1/2} \qquad (E = \text{modulus}, \rho = \text{density})$$

With appropriate constants this yields:

$$l\,(\text{nm}) = \frac{317}{\nu\,(\text{cm}^{-1})}$$

which was found both adequate and accurate as checked against the extended form of paraffins, in this case of accurately known length. It is in this way that l values equal to extended chain length L (denoted E-form) and to integer fractions thereof (IF-forms), such as once-folded (two stems of length $L/2$, to be denoted F2) twice-folded (three stems of length $L/3$, F3) etc. were obtained. SAXS measurements provided Bragg spacings (d) corresponding to layer stacking. Such d values were either equal to, or in some cases slightly (by a few per cent) larger than the l values obtained from LAM. Alternatively, they could be significantly smaller, consistently by around 18%, than the LAM based l values. The first case was interpreted as chains or stems being perpendicular (to be denoted $E_\perp$, $F_\perp$ etc.) and the second as being inclined to it ($E_\angle$, $F_\angle$ etc.). Perpendicular structures were observed in solution grown crystals while oblique structures were obtained from the melt. This is in broad agreement with the behaviour of paraffins with more than *ca.* 30 carbon atoms[12,13]. Defined in the manner described above, the inclination angle (with relation to layer normal) in the oblique structures was found to be close to 35° which corresponds to a basal plane of {201}. The latter is very plausible, as it is the most frequently observed obliquity in polyethylene and also the one to which shorter paraffins converge with increasing temperature in the so-called high-temperature monoclinic form[13].

Raman LAM spectroscopy cannot be readily applied to the present *in-situ* crystallization experiments since, (a) the spectra cannot be recorded rapidly enough, (b) the spectral interpretation becomes less straightforward as the melting temperature is approached. For this reason, in the present work we shall need to rely mainly on SAXS.

Scope of present work

The principal novelty of the present work is the recognition of a transient state with non-integral fold length as the product of primary crystallization, detected so far at temperatures below the melting point of the once-folded form. This primary state transforms subsequently to one with either larger or smaller l, the latter two being clearly states of greater relative stability and correspond to the final products identified as E and F2 in ref. 1. There is some latitude in classifiction according to spacings because the l values of the stable transformation products themselves shift with temperature by a few per cent, and this in a reversible manner, an effect not yet fully explored. Nevertheless, we tend to identify the latter as the E and F2 states even at elevated temperatures. Accordingly, we identify the transient state having l values significantly different from the integer reciprocals of the extended chain length as the non-integer form (NIF). This newly recognized transient NIF state is distinct also in respects other than l values. Thus it is prone to transform, has high X-ray diffraction intensity at low angles and is also distinct regarding crystallization rates and annealing behaviour. In the course of the paper experimental evidence leading to the above recognitions will be presented. This will be followed with some generalizations regarding their significance for chain folded crystallization to be developed in more explicit terms in a separate note[14].

EXPERIMENTAL

Materials

We chose for the present work $C_{246}H_{494}$ as most representative of the range between typical short chain paraffins and chain-folded polymers, and available in sufficient quantity for a comprehensive investigation. Even so, for any given experiment we were restricted to a few milligrams. All the *in situ* crystallization studies were as from the melt.

Measurement techniques

Synchrotron X-ray diffraction. The experiments for following crystallization *in situ* were performed on the Daresbury Synchrotron Radiation Source using a focussed (both horizontally and vertically) monochromatized beam of wavelength 0.1608 nm. The beam had a cross-section of 1×0.3 mm in the sample plane. Sample-to-detector distance was in excess of 2 m. One-dimensional position sensitive detection was used. The data aquisition system was capable of storing 256 successive time frames.

The sample was contained in a 1 mm Lindemann glass capillary held within a modified Mettler hot stage with temperature control within 0.1°C, the absolute scale having been cross-calibrated with d.s.c. For isothermal experiments the specimen stage was allowed to cool freely from above the melting point to the preset temperature. Independent calibration established this cooling rate to be 1/4°C/s. Fully isothermal conditions were established approximately 20 s after the preset temperature was reached with the initial overshoot of less than 0.5°C.

All of the X-ray beam was passed through the centre of the specimen which was achieved by remotely controlled alignment. The alignment was carried out while both monitoring the beam attenuation by means of an ion chamber behind the specimen, and while recording successive scattering curves. The long dimension of the beam was parallel to the capillary. The primary beam intensity was monitored and corrected for variations throughout. No slit desmearing was found necessary. Unless stated otherwise, the traces to be shown below represent intensities *versus* $s \equiv (4\pi \sin\theta)/\lambda$ after correction for detector response, background subtraction and Lorentz correction.

Other techniques

l values were obtained also by Raman LAM spectroscopy in a few selected cases when the sample was cooled to room temperature after the appropriate crystallization treatment. A triple monochromator Coderg spectrometer was used. The crystallization behaviour was also mapped calorimetrically using Perkin–Elmer DSC 2 and DSC 1B instruments.

RESULTS

Experimental scheme

The experiments will be presented in the following sequence. First some room temperature l values for $C_{246}H_{494}$ will be quoted as general background. Then, crystallization will be followed on cooling from the melt which reveals the various effects that can take place. In order to isolate the individual processes subsequent experiments are conducted isothermally at chosen temperatures of which three examples will be presented. Following this we shall attempt to quench the structure at an intermediate state of transformation and then follow it on reheating.

Room temperature l values for $C_{246}H_{494}$

From present and previous works[1] the l values of $C_{246}H_{494}$, and the structure types assigned, (bearing in mind that the chain length is $(246 \times 0.1273) + 0.2 = 31.5$ nm) are as follows.

Solution crystallization. Solution crystallization on cooling from petroleum ether (as obtained on synthesis): by LAM $l = 10.4$ nm; by SAXS $d \equiv l = 10.5$ nm. This identifies the structure practically as an exact $F3_{\perp}$. In some preparations F4 was also identifiable.

Crystallization from the melt. At supercoolings up to 15°C with relation to T_m(E): By LAM $l = 31.7$ nm; by SAXS $d = 25.7$ nm, which, by $d/\cos 35° = 31.3$ nm, identifies the $E_{\angle}$ structure.

Crystallization during cooling. At moderate rate (i.e. *ca.* 2 deg/min): By LAM $l = 15.8$ nm which identifies crystal as F2; by SAXS $d = 13.3$ nm which, by $d/\cos 35° = 16.2$ nm, identifies structure as $F2_{\angle}$.

Cooling at fast rate. By LAM $l = 15.7$ nm; by SAXS: broad first order peak centred on $d = 16.2$ nm, which appears to be a superposition of two sometimes possibly even three closely spaced components; at present this is tentatively ascribed to an $F2_{\perp}$ structure containing a variable fraction of $F2_{\angle}$. (Note: both here, and in the previous case above, l_{SAXS} is slightly larger (by about 3%) than $l_{LAM} \equiv l_{calc.}$).

Constant cooling rate experiments

Figure 1 displays a series of scattering curves taken at 30 s (0.5°C) intervals during cooling of $C_{246}H_{494}$ from the melt at a constant rate of 1°C/min. First to appear is a very weak reflection at 25.7 nm (just about detectable in *Figure 1*) which corresponds to the $E_{\angle}$ form. This is followed below 121°C by a peak at a larger scattering angle (corresponding to 21.3 nm) increasing rapidly in size on further cooling to become by far the most intense peak in the series of patterns. This we identify as being due to the non-integer form (NIF), i.e. a form with l differing significantly from the exact integral reciprocal of L. Below 118°C the NIF peak intensity decreases becoming a mere shoulder and finally disappearing at still lower temperatures (see below). Throughout the lifetime of NIF the spacing of this structure continuously decreases, as is most readily noticeable by the drift in the second order NIF reflection. As NIF disappears, two new forms appear, $E_{\angle}$ and $F2_{\angle}$, with the first order peaks at 25.9 nm and 14.0 nm, respectively (for further comments on the assignment of the $F2_{\angle}$ peak see below).*

We thus see that the newly identified NIF is transient, some of the corresponding crystals transforming into the thicker E, some into the thinner F2 within the time and temperature interval embraced by the experiment in *Figure 1*.

At the stage when room temperature is reached the NIF peak is reduced below detection level and only $E_{\angle}$ and $F2_{\angle}$ remain, this time in exact integer ratios of l's. *Figure 2* is a Raman LAM spectrum which, this time at

* Traces such as *Figure 1* raise the issue of overlapping orders. Thus the second order of E will be indistinguishable regarding the angular position from the first order of F2 and so on. In most instances (e.g. *Figure 1*) such a distinction can nevertheless be made on intensity grounds, as a second order is certainly not expected to be stronger than the first. The latter is the case in *Figure 1* where thus $F2_{\angle}$ is clearly identified, while some residual doubt may still persist in *Figure 6*. Even where the second order $E_{\angle}$ peak is weaker than the first order one, the presence of a sizeable fraction of $F2_{\angle}$ can be detected due to its somewhat larger d-spacing (by a fraction of a nanometer). This potential uncertainty is totally removed whenever LAM spectrum can be recorded.

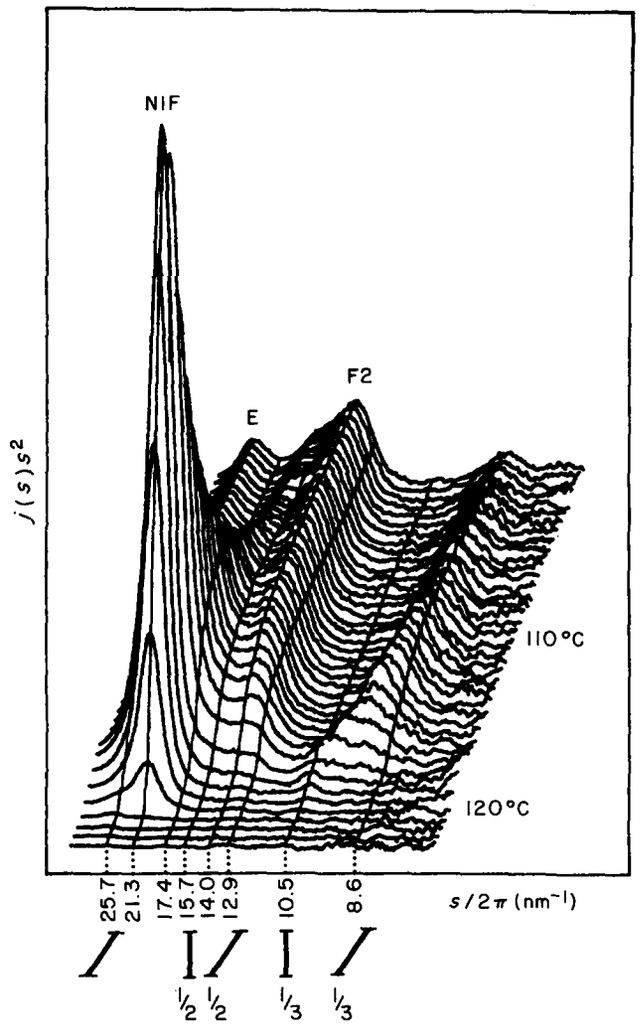

Figure 1 Series of X-ray scattering curves recorded at 30 s (0.5°C) intervals during cooling the paraffin $C_{246}H_{494}$ from the melt at a constant rate of 1°C/min. The curves are background-subtracted and Lorentz-corrected. Abscissa scale is linear in $s=(4\pi\sin\theta)/\lambda$. Characteristic $s/2\pi$ values (in nm^{-1}) are marked corresponding to the ideal layer periodicity for extended chains tilted by 35° and integer fractions, one half ($I_{1/2}$) and one third ($I_{1/3}$), as well as for one half ($I_{1/2}$) and one third ($I_{1/3}$) the layer periodicity for perpendicular extended chains. The first order diffraction peaks due to the non-integer form (NIF) and the two integer forms $E_{\perp}$ and $F2_{\perp}$ are indicated. The second-order NIF peak first appears at 10.5 nm, then shifts to smaller spacings and finally merges with the third-order $E_{\perp}$ peak at 8.6 nm. In later curves the second order $E_{\perp}$ peak at 13 nm is unresolved from the more intense $F2_{\perp}$ peak at 14 nm

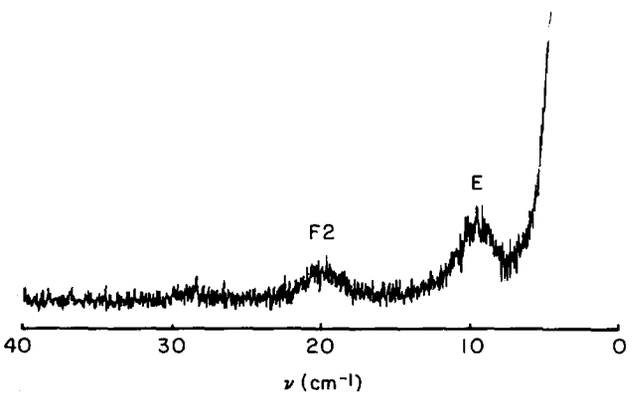

Figure 2 Raman longitudinal acoustic mode (LAM) spectrum of $C_{246}H_{494}$ sample after cooling from the melt at 1°C/min, i.e. after a cycle identical to that recorded in *Figure 1*. Only modes corresponding exactly to E and F2 forms are present: first-order modes at $\nu=10.0\,cm^{-1}$ and $20.0\,cm^{-1}$ give $l_{LAM}=15.8$ nm and 31.7 nm, respectively. The weak third order E mode at $29\,cm^{-1}$ is also visible.

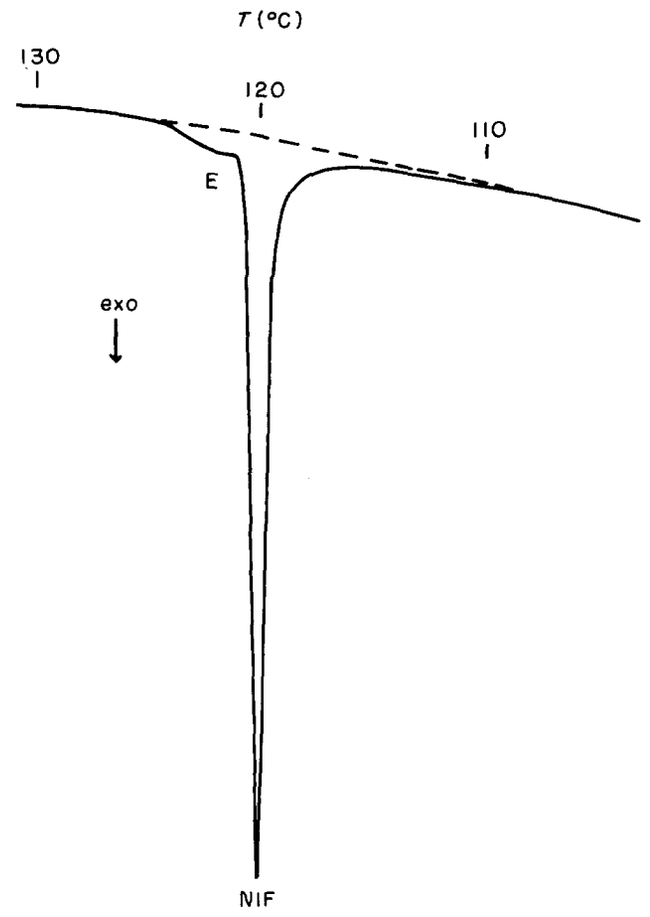

Figure 3 D.s.c. cooling scan recorded at 1°C/min, showing melt crystallization of $C_{246}H_{494}$ (cf. *Figure 1*). Exotherms due to crystallization of the E and NIF forms are indicated

room temperature, can be readily used to identify the two structures present simultaneously without ambiguities regarding obliquities and diffraction orders. Only odd modes are Raman active, and indeed the third order mode of E is just about identifiable in agreement with the above structure assignment.*

Figure 1 should be compared with *Figure 3* which shows a d.s.c. cooling scan of $C_{246}H_{494}$ at the same cooling rate of 1°C/min. First, at 125°C a small exotherm starts appearing which is due to the onset of extended-chain crystallization. The large sharp exotherm below 121°C corresponds to the rapid crystallization of NIF. We notice in passing the unusual phenomenon of slowing down in the extended-chain crystallization range as the NIF growth transition temperature is approached from above. This effect will be the starting point of a separate announcement to follow shortly[8]. For the present purposes it suffices to say that the distinctness of, what we now identify as NIF structure becomes apparent also through the crystallization rates.

Isothermal experiments

Based on the cooling experiments we selected appropriate temperatures for isothermal crystallization so as to obtain

* Asymmetric folding into two stems of non-equal length such as envisaged in a NIF structure, would be expected to result in broadening of the F2 LAM peak if stems are fully elongated; or alternatively, if there were cilia forming an amorphous layer, the average LAM frequency would be increased with respect to that corresponding to half the extended chain length. The spectrum in *Figure 2* shows neither of the above two indications of the presence of an appreciable fraction of NIF.

the thickening and thinning processes on their own, expecting the former to occur at the higher, the latter at lower temperatures within the temperature range covered by *Figures 1* and *3*.

Figure 4 corresponds to crystallization at the higher temperature of 120.5°C and shows an example of NIF→E transformation now occurring isothermally. As seen, the initial intense NIF peak shifts to lower s values corresponding to the $E_{\perp}$ structure. Judging from the fact that the central scatter passes through a maximum at 3 min, apparent from the display of the SAXS curves as in *Figure 5*, and from the details of the development of the relative peak intensities (not itemised here) it is concluded that the thickening of the NIF structure is on the time scale of the primary crystallization. Specifically, all of the specimen becomes crystalline after about 7 min. This is also consistent with the crystallization rates[8] (also *Figures 1* and *3*).

Figure 6 displays traces of isothermal recording at the somewhat lower temperature of 117.8°C. The main points observed are: (a) The primary crystallization product is again a transient which transforms subsequently. (b) In view of the fact that here primary crystallization into NIF is much faster than for 120.5°C (see *Figures 1* and *3*) most of the material will be largely crystalline by the time the first scattering curve is recorded. Hence, the transformations recorded are within an essentially fully crystallized material in the sense that no separate molten phase is present. (c) The thickening (NIF→E) itself is slower than at 120.5°C. It follows that NIF has a correspondingly longer lifetime during which, now at the lower temperature of 117.8°C, continuous isothermal reduction in spacing of NIF, as yet untransformed to E, also takes place. (d) The appearance of discrete E peaks simultaneously with a continuous thinning of the remaining NIF lamellae strongly suggests that chain extension proceeds by nucleated transformation. The transformation is complete after 15 min at 117.8°C.

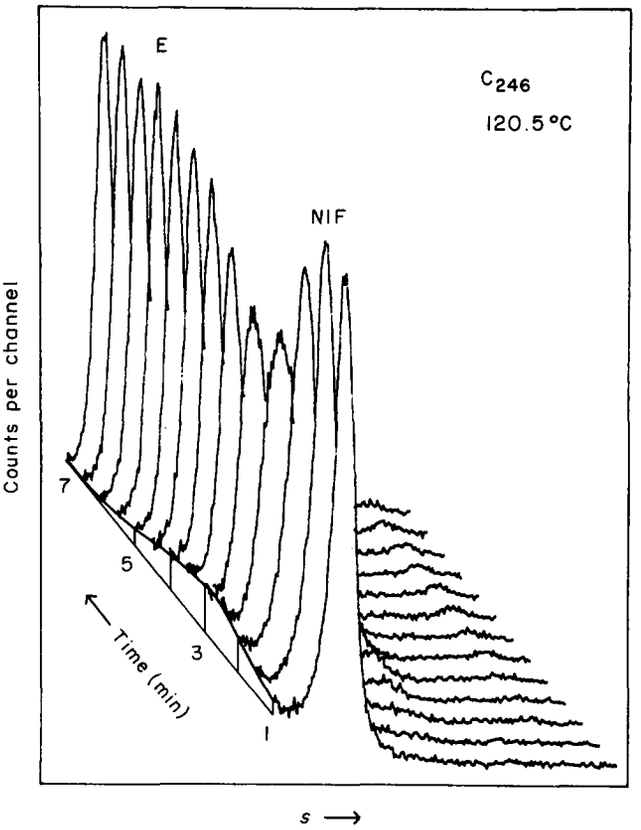

Figure 5 Scattering curves of the same 120.5°C crystallization run as in *Figure 4* but without Lorentz correction. This is to show that the central scatter passes through a maximum at $t = 3$ min giving a rough measure of the half-time of crystallization. By $t = 7$ min crystallization is virtually complete

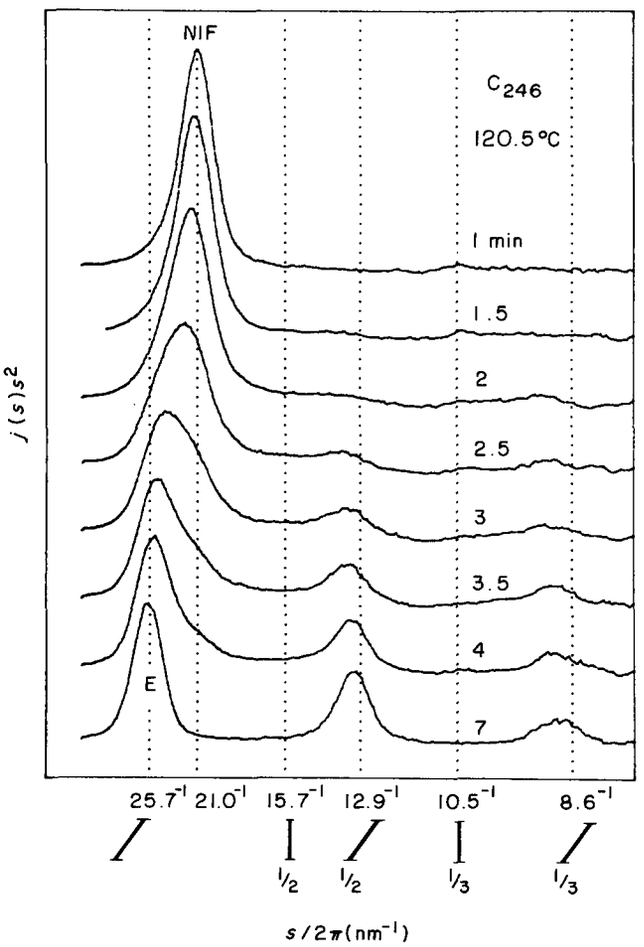

Figure 4 Series of X-ray scattering curves recorded during isothermal crystallization of $C_{246}H_{494}$ at 120.5°C. Time (in minutes) after reaching the crystallization temperature is marked for each curve. Thickening of the NIF lamellae occurs immediately after their formation. The end result is the pure $E_{\perp}$ form of which 3 diffraction orders can be seen in the bottom curves

At the substantially lower temperature of 106°C (*Figure 7*) we see again the intense NIF peak first, gradually giving way to a peak at a larger scattering angle, hence smaller spacing, which we now assign to a $F2_{\perp}$ structure. Here again the NIF diffraction peak becomes very much reduced with time but does not disappear completely even after 33 min. No thickening occurs at this temperature. It can again be inferred from the known rates (ref. 8 and *Figures 1* and *3*) that by the time the first trace is recorded, after 0.2 min at 106°C, primary crystallization is complete, hence the sequence of traces in *Figure 7* represents transformation within the fully crystallized material.

Figure 7 also shows the effect of cooling of this fully crystallized sample to 45°C. Both the reduction in scattering intensity and the shift of the $F2_{\perp}$ peak towards lower spacing, hence closer to exact correspondence to the expected $F2_{\perp}$ value, is apparent. These latter, temperature induced changes are reversible; the final pattern at 106°C (the 33 min trace) is regained again on

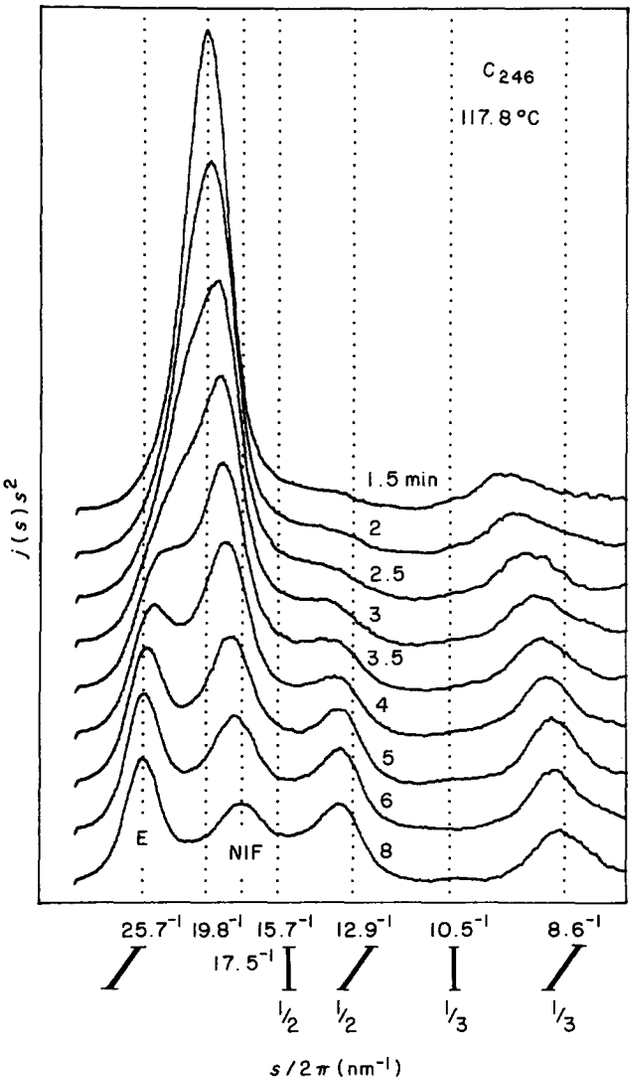

Figure 6 Series of scattering curves of $C_{246}H_{494}$ recorded at the constant temperature of 117.8°C. Time t (in minutes), after reaching this temperature on cooling from the melt, is indicated for each curve. The primary crystallization in the NIF form is virtually complete by the time the first curve is recorded. Subsequent changes in the solid involve two processes clearly visible in the Figure: (a) chain extension by what appears to be a nucleated transformation into the $E_{\angle}$ form, and (b) the remaining untransformed NIF undergoes a continuous reduction in layer periodicity by *ca.* 2.5 nm in the period of $6\frac{1}{2}$ min

heating up from 45°C. The very much greater reversible temperature dependence of the NIF peak intensity, compared with F2, is to be noted (also see below).

In summary, *Figures 4–7* reveal that the NIF structure represents the primary process of crystallization; it then reorganizes by isothermal thickening into E, or by isothermal thinning into F2, with details differing at different crystallization temperatures (T_c).

The l values (or rather d spacings) for the primary NIF structures deserve comment. They vary with T_c, higher T_c values yielding higher l values, the range in *Figures 4–7* being 18.5–21.4 nm. This range is near the F2 end of the F2–E interval. NIF peak closer to E could not be obtained on direct crystallization: T_c only a degree higher than in *Figure 4* gave no NIF, only E peaks. It should be remarked that the lowest temperature at which crystallization actually took place in the present work could have been in the range of 115°C. This limit to supercooling was, on the one hand, due to the very rapid crystallization of NIF, only a couple of degrees below its maximum crystallization temperature of 121°C, and, on the other hand, to the limited cooling rate which could be employed with the specimen holder used. Thus the lowest recorded spacings of the as-formed NIF does not necessarily represent the lower limit obtainable.

Freezing in of the NIF structures; effect of subsequent heating

The preservation of NIF, so far observed as a transient at elevated temperatures, would clearly be of interest. However, on relatively slow cooling the NIF transforms into E or F2 or both, as already stated. It was also mentioned earlier that by rapidly cooling the melt broad reflections are observed, the centre of the first order reflection corresponding to 16.2 nm. Since $l_{LAM} = 15.8\,\text{nm} = L/2$ in this case, the resulting form is denoted as $F2_{\perp}$. It is not clear at present whether $F2_{\perp}$ represents the lower end of NIF with continuously varying l, or whether a discontinuity between $F2_{\perp}$ and NIF exists. Presently we are inclined to believe that the former is the case, which would also imply that chains are perpendicular in NIF layers. As mentioned above, the high temperature coefficient of NIF crystallization rate

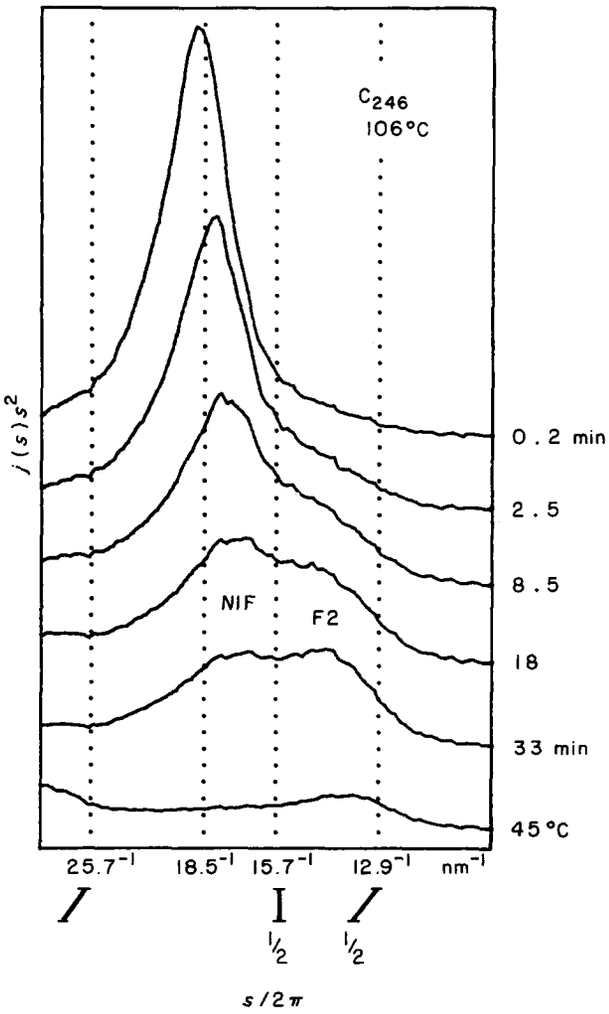

Figure 7 Series of scattering curves of $C_{246}H_{494}$ recorded at the constant temperature of 106°C. t (in minutes) is indicated. The primary crystal form is again NIF ($d = 18.8$ nm). Lamellar thinning, both continuous (to $d = 17.5$ nm) and discontinuous (to the tilted F2 form, $d = 14.0$ nm) take place at this lower temperature. The bottom curve is taken at 45°C immediately after recording the 33 min curve at 106°C

(dr_{NIF}/dT), indicates that even on quenching the crystallization must have actually taken place at a relatively small supercooling, which is also the reason that no F3 form was observed on melt quenching. (From rapid d.s.c. scans of solution-grown $C_{246}H_{494}$ crystals the melting point of the F3 form was determined to be 113°C ± 1.5°C).

When the cooling rates were between 10°C–20°C/min two clearly resolved first-order SAXS peaks were observed at room temperature, one corresponding to the $F2_{\perp}$ form (13.3 nm) and the other to what may be classified as NIF (18.0 nm) (see top curve in *Figure 8*). Similar results, but using higher cooling rates, were also observed with the paraffin $C_{198}H_{398}$, where, rather remarkably, significant reduction in spacing of the frozen NIF form occurred on storage at room temperature: the reduction was from 15.4 to 13.0 ± 0.4 nm, the latter value being close to 12.7 nm calculated for the ideal $F2_{\perp}$ form. Incidentally, this NIF→F2 transformation also suggests that the chains are perpendicular in NIF since, in line with the experience with short paraffins, it is unlikely that the large cooperative motion associated with the change of tilt would occur at room temperature.

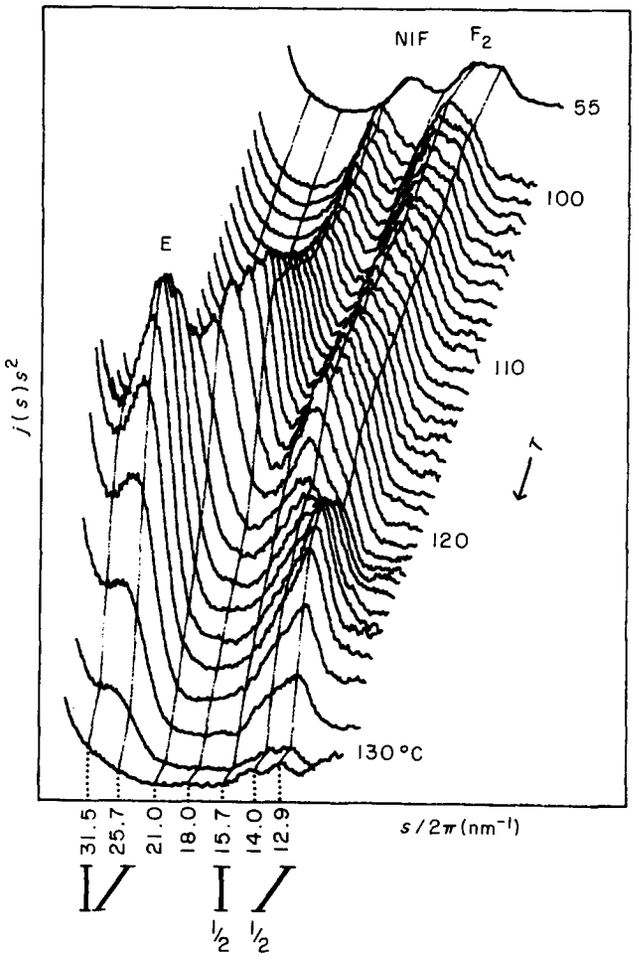

Figure 8 Series of scattering curves recorded at 1°C intervals during heating a 'mixed' sample of $C_{246}H_{494}$ containing both NIF and $F2_{\perp}$ forms. The separate uppermost curve is recorded at 55°C. The paraffin had been crystallized by cooling the melt at approximately 15°C/min (in this particular preparation it appears that the '$F2_{\perp}$' peak itself is a doublet comprised of a sharper component at 13.0 nm and a broader one at *ca.* 14.2 nm; however for the present purpose we shall treat the two together as $F2_{\perp}$). On heating both peaks increase in intensity and spacing, but the increase is much larger for NIF than for $F2_{\perp}$. At *ca.* 122°C both forms give way to the $E_{\perp}$ form of which two diffraction orders are visible

Significant effects are being observed in ongoing work involving the heating up of 'mixed' samples from room temperature to the melting point while following diffraction behaviour *in situ*. *Figure 8* shows one example.

The principal features we are drawing attention to here are as follows: (a) NIF and $F2_{\perp}$ remain separate entities throughout the heating run. (b) While the spacing and the diffraction intensities of both form increase with temperature, the extent to which this occurs shows qualitative differences. The increase in the first-order peak intensity is much larger for NIF: between 55°C and 121°C the integral intensity increases by a factor of 8.2 for NIF and only 2.7 for $F2_{\perp}$. In the same temperature interval the spacings of $F2_{\perp}$ increases only by 0.5 nm, while that of NIF increases by 4 nm. (c) Both forms eventually give way to $E_{\perp}$ at the same temperature of 122.5 ± 1.5°C. For comparison the E form melts at 128.6°C, as determined by d.s.c.

At the relatively slow heating rate (3°C/min) employed in the experiment in *Figure 8* it is not certain as to what extent the transformation to $E_{\perp}$ involves melting. However, heating runs performed at higher rates leave little doubt that melting is the primary process. In fact at heating rates above *ca.* 50 deg/min no E form appears at all as there is no time for recrystallization from the melt. Also at the higher rate of heating the NIF lamellae thicken to a lesser extent than on slow heating and the resulting thinner NIF structures melt at correspondingly lower temperatures. This allows a closer estimate of the melting points of the primary unaltered NIF structure which is thus found to be 1–2°C lower than that ofthe $F2_{\perp}$ form. This is important information to be referred to in the Discussion section. A detailed account of the melting process will be presented in a separate publication.

DISCUSSION

The main new findings

As already stated in the preliminaries the principal experimental result is the recognition that primary crystallization yields l values which are non-integer fractions (NIF) of the chain length. Nevertheless, this is only a transient stage transforming into the integer fraction (IF) state still during crystallization or during cooling or both. The transformation itself can occur either by thickening or, rather remarkably, by thinning into the nearest IF state. This is represented schematically by *Figure 9*. It follows immediately that the closely IF structures reported previously[1] represent already transformed and not the initial structures, and thus all the conclusions reached so far apply only to these transformed structures, at least in the direct manner there stated.

On l *values*

The primary l values from the new results now depart from the strict quantization claimed previously before the transient NIF state was recognized. The actual l values display a certain continuity with T_c, somewhat in a manner as in polyethylene, higher T_c yielding larger l. Nevertheless this apparently continuous range of primary l values is confined to the F2 side of the E–F2 range, there being a sizeable gap in primary values on the E side of the range. We believe that this gap is genuine and not due to NIF structures in this range transforming into E so

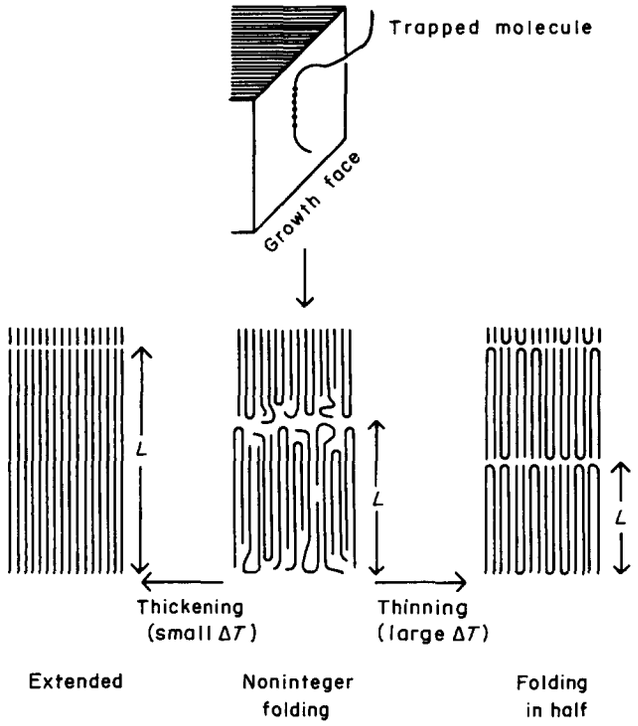

Figure 9 A schematic representation of primary NIF crystallization and subsequent changes into IF structures in the crystallization temperature range $T_m(F2) < T_c < T_m(E)$

rapidly that they escape detection, as might be surmised on the basis that increasing proximity of the E state would accelerate the transformation in the upward direction. This contention is based on the finding that the crystallization rate in the NIF form and its temperature dependence are distinct from that of the E state and *vice versa* (*Figure 3*). If part of what we now identify as E range were initiated by an undetected NIF structure this situation could not arise, because then the formation of NIF would remain the rate determining factor.

On the fold surface structure

The regularity of the fold surface has been inferred previously through evidence from room temperature measurements on IF structures[1] which, as we now recognize, are products of refolding. While it should not detract from the importance of the fact that such sharp fold structures, as inferred in ref. 1, can exist, in fact all our systems tend towards them by rearranging accordingly, we now have strong indications that the primary fold structures are more disordered than the ones into which they transform. There are in fact two factors at play. One is the reversible temperature dependence of the fold structure even in the rearranged IF state indicated by the change both in intensity and spacing with temperature. The increased intensity at the higher temperature implies greater electron density deficiency at the interface, hence increased looseness of structure. This we do not follow up here because it is far surpassed by the second feature, the high scattering intensity of the NIF phase, as compared with the IF state, particularly at elevated temperatures. A statement on this feature follows.

Measurements of absolute diffraction intensities can provide quantitative information about the structure of the interlamellar layers. Even though we did not measure intensities in absolute units, by comparing the intensities of different diffraction orders from different crystal forms we could obtain the ratios of interlayer parameters for different states. Thus, using the approximate method due to Strobl[15] we compared the NIF and $E_\perp$ structures, both at the same temperature of 106°C. The two parameters derived by the above method are κ, the total electron density deficiency of the interlayer with respect to the density of the crystalline layer (the zeroth moment) and σ^2, the second moment of the distribution of this deficiency along the layer normal. Our comparison resulted in the following two ratios at 106°C: $\kappa_{NIF}/\kappa_E = 2.1$; $\sigma_{NIF}/\sigma_E = 1.8$. In broad terms this can be interpreted as the NIF surface layers containing twice as much disordered material as those of the $E_\perp$ form.

It should be noted that the above comparison was made at elevated temperatures where there is considerable disorder at the layer surface even in the E form as compared with the ordered modifications determined previously in shorter alkanes[16,17]. This is apparent from the fact that the diffraction intensity of the E form is significantly reduced on cooling to room temperature which in turn indicates a reduction in κ. Even at room temperature, since the chains are tilted in the melt-crystallized $E_\perp$ form, the end-groups are not in crystallographic register; the order could at best be of the type encountered in the high-temperature monoclinic (C-type)[12,13] modification of shorter paraffins.

On the origin of NIF structures

The issue invites extensive discussion. At this place, so as not to detract too much from the experimental message of the work, only a very brief outline will be given of a line of argument which will be made more explicit in a subsequent paper[14].

The issues in question hinge on two competing criteria, those of maximum stability and fastest kinetic pathway, which in turn take us back to the basis of chain folding itself. It is now accepted that the state of maximum crystal stability for polymers in general is that of the fully extended chain, and chain-folding arises because it is in this way that the crystal can grow fastest. The resulting crystal is in a state of lower than maximum stability, and the more so the shorter l (surface free energy term is inversely proportional to l). Nevertheless it will tend to the state of maximum stability via refolding whenever mobility conditions permit, which can apply at the crystallization temperature itself (isothermal thickening) or may set in on raising the temperature (heat annealing). The same will apply if the chains are short and strictly uniform, only now additional local minima in free energy will arise for l values corresponding to integer fractions of the chain length when the chain ends will all be at the layer surface. When the IF values were first observed in our uniform paraffins[1], as indeed in preceding works on PEO of narrow molecular weight distribution, it was believed implicitly or explicitly (e.g. ref. 18) that it is these states of local stability corresponding to IF which modify the usual kinetics and thus determine the actual primary l values. The present recognition of NIF states means that this is not so and that the kinetics favours other pathways despite the greater ultimate stability of the IF structures (themselves of course being only states of enhanced stability within the intrinsically metastable spectrum of folded structures). And just as conventional chain-folded structures tend towards the stablest E structure by

refolding, so do the primary NIF structures in our paraffins but now taking note of the nearby IF structures as stations of increased stability along the road towards E, which in this case can comprise also lowering of l values, i.e. thinning. The latter implies that the melting point of F2 is higher than that of the relevant NIF transforming into it. We have seen that this indeed is the case.

Next, one may ask why should the pathway to NIF be kinetically favoured over that leading to the nearest IF state? The reason for this is clearly perceived even qualitatively, at the same time highlighting a pertinent factor not normally taken account of in crystallization theories involving chain folding.

Consider a chain depositing along the crystal face as in *Figure 9*. It will be apparent that without translation the particular chain, as drawn there, will not be able to complete an IF structure, neither E nor F2. For these the position of the first attachment has to satisfy very special conditions with correspondingly low attachment probability. Thus the probability of a depositing chain leading to NIF will be much higher than that leading to IF, from which it follows that NIF will be the pathway for faster growth.

It will be seen further that random attachment such as in *Figure 9* (top), will result in defects within the crystal and in disorder at the layer interface. The resulting structure is in qualitative agreement with the observed increased density deficiency in NIF of interlamellar layers. The above issue of initial deposition probability does not normally feature in theories of chain folding in case of long chains but will become the rate determining factor, a kind of entropic barrier[23], for the present long alkanes. This will be discussed, together with the structure of NIF state, more specifically in a paper to follow[14]. At this point only that much will be stated that our uniform alkanes now present us with an opportunity to probe the stage of the initial chain deposition, not achievable previously.

Relevance to polymers

The main issues have been stated in ref. 1, to which the present work has further substantial points to add. These are:

(1) The l values as formed are transient, subsequently transforming into the stabler final structures. This has its counterpart in polyethylene (PE) (for most recent results see ref. 19), except that in the latter the transformation is in the upward direction only.

(2) In polyethylene the l values themselves are a continuous function of T_c (or ΔT) while, as assessed in the final state, the present alkanes display quantized values. Nevertheless, the present work shows that, when forming, l can have values in between the previously noted quantization even if not spanning the full range, thus at least approaching the behaviour of PE.

(3) In the alkanes the folds, when forming, must have appreciable looseness but become sharp after refolding and cooling. The nature of the fold, whether loose or sharp, has been a major issue in high polymers, studied most closely on PE. We now see on our model alkanes that both loose and sharp folds can occur, in this case in a more precisely documentable manner than was possible with PE, and further, that exactly which state is observed depends on the stage of crystallization and/or transformation at which the system is examined. This places the fold surface structure issue in a new light, in as far as it demonstrates that no categoric statement can be made from examination of just any one specimen. Beyond this, our work on alkanes now created a situation where the conditions under which one or the other type of structure is obtained can be controlled. In the light of the above the originally conflicting findings of Lee and Wegner[9] on similar long alkanes, might perhaps be reconcilable with our own results. It is to be noted that in the alkanes the fold surface disorder, when it occurs, must still be confined to loops spanning nearby, if not adjacent stems. In addition to this kind of loose loop, in the case of high polymers truly wide loops such as bridge distant portions of the same molecule which may have started to form their own chain folded deposition would need counting with. The latter would thus form an additional source of disorder, and would not be so readily removable by isothermal refolding and/or by cooling to room temperature.

As laid out in ref. 1 the question of when and how short chains start folding and how such folding occurs is a long standing issue. Some of the more recent works are mentioned in the Introduction. Others of various degrees of definiteness are spread over 25 years of literature. This is not the place to review them beyond stating that such apparently conflicting models where the chain ends are always at the fold surface[5,7] and where fractional stems fold back into the crystals[20,21] feature in it. The present work now shows that either of these models can pertain pending on whether primary or transformed structures are being considered.

Finally, an issue underlying all the present work is the high mobility of the chain within the crystal lattice. This should be highly relevant, not only to the crystallization itself, but to the structure of the crystals and to the dynamics of the chain in the solid state with all its consequences for properties. This mobility should also be highly pertinent to the behaviour of conventional short paraffins where correspondingly high mobility has been deduced by ourselves previously through diagnozing bodily movement over microscopic or even macroscopic distances of entire chains while still in the crystal[22].

ACKNOWLEDGEMENTS

We are greatly indebeted to Professor M. C. Whiting and Dr I. Bidd (Organic Chemistry, Bristol) for having developed the synthesis of these ultra long alkanes and for providing us with the materials which made this work possible. Additionally we would like to thank Professor Whiting for his constructive interest throughout the work. One of us, G.U., wishes to acknowledge financial support from the Science and Engineering Research Council.

REFERENCES

1 Ungar, G., Stejny, J., Keller, A., Bidd, I. and Whiting, M. C. *Science* 1985, **229**, 386
2 Paynter, O. I., Simmonds, D. J. and Whiting, M. C. *J. Chem. Soc., Chem. Commun.* 1982, 1165; Bidd, I. and Whiting, M. C. *ibid.* 1985, 543
3 Arlie, J. P., Spegt, P. and Skoulios, A. *Makromol. Chem.* 1967, **104**, 212
4 Kovacs, A. J. and Straupe, C. *Faraday Disc.* 1979, **68**, 225

5 Sadler, D. M. and Keller, A. *Kolloid Z. Z. Polym.* 1970, **242**, 1081
6 Leung, W. M., St. John Manley, R. and Panaras, A. R. *Macromolecules* 1985, **18**, 746
7 Buckley, C. P. and Kovacs, A. J. in 'Structure of Crystalline Polymers', (Ed. I. H. Hall), Elsevier, Applied Science Publishers, 1984, p. 261
8 Ungar, G. and Keller, A., submitted to *Polymer*
9 Lee, K. S. and Wegner, G. *Makromol. Chem., Rapid Commun.* 1985, **6**, 203
10 Yeates, S. G. and Booth, C. *Makromol. Chem.* 1985, **186**, 2663
11 Schaufele, R. F. and Shimanouchi, T. *J. Chem. Phys.* 1967, **47**, 3605
12 Strobl, G. R., Ewen, B., Fischer, E. W. and Piesczek, R. W. *J. Chem. Phys.* 1974, **61**, 5257
13 Takamizawa, K., Ogawa, Y. and Oyama, T. *Polym. J.* 1982, **14**, 441
14 Ungar, G., to be published
15 Strobl, G. R. *Kolloid Z. Z. Polym.* 1972, **250**, 1039
16 Smith, A. E. *J. Chem. Phys.* 1953, **21**, 2229
17 Shearer, H. M. M. and Vand, V. *Acta Crystallogr.* 1956, **9**, 370
18 Hoffman, J. D. *Polymer* 1986, **27** (*Commun.*), 39
19 Martinez-Salazar, J., Barham, P. J. and Keller, A. *J. Mater. Sci.* 1985, **20**, 1616
20 Balta-Calleja, F. J. and Keller, A. *J. Polym. Sci., A-2* 1963, **2**, 2151
21 Zahn, H. and Pieper, W. *Kolloid Z. Z. Polym.* 1962, **180**, 97
22 Ungar, G. and Keller, A. *Colloid Polym. Sci.* 1979, **257**, 90
23 Sadler, D. M. *J. Polym. Sci., Polym. Phys. Edn.* 1985, **23**, 1533